Theory Underlying Measurement of AOA with a Rotating Directional Antenna

Yinjie Chen*, Zhongli Liu*, Xinwen Fu*, Benyuan Liu* and Wei Zhao‡
*University of Massachusetts Lowell, Email: {ychen1, zliu, xinwenfu, bliu}@cs.uml.edu
‡University of Macau, Macau, China, Email: weizhao@umac.mo

***Abstract*—In many wireless localization applications, we rotate a directional antenna to derive the angle of arrival (AOA) of wireless signals transmitted from a target mobile device. The AOA corresponds to the direction in which the maximum received signal strength (RSS) is sensed. However, an unanswered question is how to make sure the directional antenna picks up packets producing the maximum RSS while rotating. We propose a set of novel RSS sampling theory to answer this question. We recognize the process that a directional antenna measures RSS of wireless packets while rotating as the process that the radiation pattern of the directional antenna is sampled. Therefore, if RSS samples can reconstruct the antenna's radiation pattern, the direction corresponding to the peak of the radiation pattern is the AOA of the target. We derive mathematical models to determine the RSS sampling rate given the target's packet transmission rate. Our RSS sampling theory is applicable to various types of directional antennas. To validate our RSS sampling theory, we developed BotLoc, which is a programmable and self-coordinated robot armed with a wireless sniffer. We conducted extensive real-world experiments and the experimental results match the theory very well. A video of BotLoc is at www.youtube.com/watch?v=WtUt0IqhXRU&feature=youtu.be.**

I. Introduction

The positioning of wireless devices with a rotating antenna is a topic that has been extensively studied in wireless networking [9], [14], [15], [21], [23]. We can rotate the directional antenna and measure the AOA of wireless signal transmitted from that mobile device. The target's AOA is the direction in which the maximum received signal strength (RSS) is sensed. When there is a line-of-sight (LOS) path between a directional antenna and a target, the maximum signal strength is sensed when the directional antenna is facing the line-of-sight direction to the target. Even if there is no line-of-sight path between a directional antenna and a target, measuring AOA is a fundamental technical problem and multiple measured AOAs can be statistically processed for accurate localization [15].

An unanswered theoretical problem is how to make sure the directional antenna picks up packets producing the maximum RSS while rotating. Intuitively, the accuracy of AOA measurement is related to angular velocity and number of rotations of the directional antenna. An extreme example is if the antenna rotates one round per second and the target's transmission rate is one packet per second, the antenna rotating is synchronized with the target packet transmission and we can never be sure whether the AOA will be measured. Experienced engineers may utilize over-sampling and rotate antenna slowly and frequently to collect as many RSS samples as possible. However, what is the underlying theory of over-sampling? Can we design optimal strategies for measuring AOA? We will address these issues in this paper.

We propose the *RSS sampling theory* to address the problem of sampling with a rotating directional antenna. We recognize the process that a directional antenna measures RSS of wireless packets while rotating as the process that the radiation pattern of the directional antenna is sampled. Therefore, if RSS samples can reconstruct the antenna's radiation pattern, the direction corresponding to the peak of the radiation pattern is the AOA of the target. Our RSS sampling theory explains the relationship between the antenna's angular velocity, number of rotations and target traffic pattern. Furthermore, we extended our RSS sampling theory to support locating targets such as laptops, tablets, and PADs, whose packet transmission intervals are irregular. We believe that our work can be applied as guidelines for designing various localization systems that use a rotating directional antenna.

Our major contributions are summarized as follows:

- We are the first to propose the RSS sampling theory for a rotating antenna (or sniffer), which can be carried by humans or vehicles, to measure AOA. We explicitly formulated the relationship between the rotating antenna's angular velocity, the target wireless device's packet transmission interval and the number of rotations. The RSS sampling theory guarantees sufficient RSS collection for precise AOA measurement and avoids over-sampling, in other words, answers what is over-sampling. We also address the cases of measuring AOA where the target transmission is irregular and unpredictable.
- We developed a fully functional AOA measurement system BotLoc, a self-coordinated robot armed with a directional antenna on top. The robot is able to rotate like a turntable with a controlled angular velocity. Therefore, the directional antenna on top of the robot also rotates and a controllable rotating antenna is formed. BotLoc applies our RSS sampling theory for collecting RSS time series and identifying the AOA of target's signal propagation. Extensive experiments are conducted with BotLoc and our results validate the correctness of all the proposed theorems.

The rest of this paper is organized as follows. We review related work in Section II. In Section III, we present the application background, and the problem definition. IV intro-

duces the RSS sampling theory. We present the localization schemes powered by the RSS samling theory via a rotating sniffer. Section V introduces BotLoc system for localization and presents experimental evaluation of BotLoc. Section VI concludes this paper.

II. Related Work

There has been a large body of work on device positioning in WiFi and sensor networks. Due to space limitation, we only review the existing work most related to our paper: Most existing techniques provide localization in a two-dimensional space (e.g., longtitude/latitude) only. Positioning systems are classified as outdoor and indoor systems, respectively, which feature vastly different requirements and techniques. The most popular outdoor positioning system is GPS [6]. Many cellular mobile networks also belong to this category, and allow the tracking of powered-on devices through the operator's base-transceiver stations. Indoor positioning systems include RADAR [2], LANDMARC [14], the digital Marauder's Map [8], Lighthouse [18], and VORBA [15]. All these systems position a mobile device based on the measured signal strength. In particular, the former three utilize a dense grid of omni-directional base stations, while the latter two rely on base stations with revolving unidirectional antennas. Active Badge [22], Active Bat [10] and Cricket [16] can provide better localization accuracy than outdoor systems due to the usage of a large number of positioning-support sensors.

In [19], the authors use electronically steerable Phocus Array antennas from Fidelity Comtech [7] for wardriving and collecting RSSIs with directional information. Multiple measurements are taken at different positions and arrows are drawn in the direction of the AP. Therefore, an AP is at the position which all the arrows point to. In [9], the authors take RSSIs from wardriving and use the gradient information derived from RSSIs to infer the position of an AP. An AP is in the direction along which RSSIs increase the most and the direction is represented by an arrow. Then the AP is at the position all arrows point to. In [13], the authors built an AP equipped with a rotating directional antenna that broadcasts its direction in beacon frames. Such an AP is denoted as a directional beaconing access point (DBAP). Therefore, a mobile may position itself by using the angle of emission information from multiple DBAPs and the area intersection approach similar to those used in [15].

In [21] Wang *et al*. present *3DLoc* which is a ground based system for locating an 802.11-compliant mobile device in a three dimensional space. However, the portability and flexibility of the system is very limited and it cannot search targets in high buildings. In [23], the authors use a human body and a smartphone as a directional antenna to locate wireless mobiles. This kind of system is portable and efficient, and applicable to outdoor localization. Chen *et al*. present very preliminary simulation results of sampling RSS for measuring AOA in their workshop paper [3].

There are also many recent works focused on indoor localization. In [4], the authors utilize the robustness and indoor penetration ability of FM signals and combine FM and WiFi signals to generate wireless fingerprints for indoor localization. Such fingerprints produce higher localization accuracy than WiFi fingerprints. In [20], the authors select indoor locations, such as an elevator, as landmarks because of the identifiable signatures they present. They develop a system UnLoc which runs on a smartphone. This system measures a user's motion using embedded sensors including accelerometer and compass and calibrates when the user crosses any landmark.

III. RSS Sampling Using a Directional Antenna

In this section, we first discuss the application background, and then define the problem of RSS sampling using a directional antenna.

A. Background

In this paper, we are concerned with measuring the target AOA with a rotating antenna by analyzing RSS samples. We now introduce how an RSS reading is measured by a directional antenna. An RSS reading corresponds to the signal strength received by the antenna, and such signal strength $P_r(d)$ can be predicted by Formula (1) [17],

$$P_r(d) = \frac{P_t G_t G_r \lambda^2}{(4\pi)^2 d^2 L}, \tag{1}$$

where $P_r(d)$ is the received power, and P_t is the transmitted power. G_t is the transmitter antenna gain, and G_r is the receiver antenna gain. d is the signal propagation distance in meters. L is the system loss factor $(L \geq 1)$, and λ is the wavelength in meters. If we measure $P_r(d)$ in dB, then we have (2),

$$10 \log P_r(d) = 10 \log \frac{P_t G_t \lambda^2}{(4\pi)^2 d^2 L} + 10 \log G_r. \tag{2}$$

The right side of Equation (2) has two parts. For the first part, in our application scenario, we rotate a directional antenna, but we do not move the antenna's position. Therefore, the distance between the transmitter and receiver is fixed, which means d does not change. Hence, the first part does not change.

Now let us consider the second part in (2). For a directional antenna, its power gain varies at different directions, as shown in Fig. 1. The variation of antenna gain over different directions incurs difference in signal reception. This means, as the antenna rotates, G_r changes, and accordingly, $P_r(d)$ changes. For example, the RSS measured by an antenna facing the LOS direction to the transmitter is much stronger than the RSS measured by the antenna pointing to the reverse of the LOS direction to the transmitter. For conciseness, we rewrite (2) as (3) for our discussion hereafter,

$$s(\theta) = P(d) + g(\theta), \tag{3}$$

where $s(\theta)$ is $10 \log P_r(d)$, and θ refers to the direction from which the signal arrives at the antenna. $P(d)$ is $10 \log \frac{P_t G_t \lambda^2}{(4\pi)^2 d^2 L}$ and $g(\theta)$ is $10 \log G_r$, as G_r varies over θ. Please note: even if there is no line-of-sight path between a directional antenna and a target, measuring the AOA is a fundamental technical

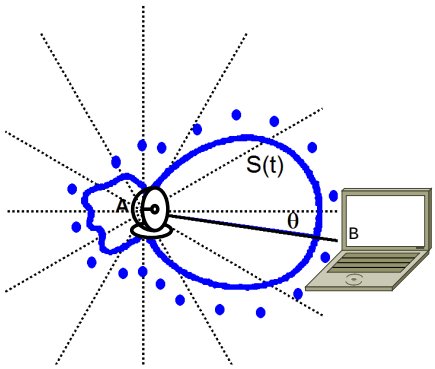

Fig. 1. Power Distribution s(t) Over Antenna's Heading

problem and multiple measured AOAs can be statistically processed for accurate localization [15].

If we plot the antenna gain over the antenna's heading, we derive its radiation pattern. The peak of this pattern corresponds to the direction with the maximum gain. Therefore, when the distance between a target and a directional antenna is fixed, a RSS received at this direction is the maximum RSS. We can model this radiation pattern as a function $g(\phi, \theta)$, ϕ is the elevation direction, and θ is the azimuth direction. Assume the antenna rotates horizontally, then ϕ does not change. Therefore, the variation of signal reception is only related to the azimuth direction θ. If the RSS samples are correctly collected, we can reconstruct the target power distribution over antenna's heading with these RSS samples, and such distribution equals the antenna power pattern over antenna heading plus a constant value.

B. Problem Definition

In many application scenarios, we need to measure AOA (angle of arrival) of a target's signal to locate the target in a space. We rotate a directional antenna to sense signals from different directions, and choose the direction where the maximum RSS is sensed as the AOA of target's signal. We recognize the process that a directional antenna measures RSS of wireless packets while rotating as the process that the radiation pattern of the directional antenna is sampled. Therefore, if RSS samples can reconstruct the antenna's radiation pattern, the direction corresponding to the peak of the radiation pattern is the AOA of the target.

Therefore, the problem of RSS sampling is defined as follows: *A rotating directional antenna, carried by a vehicle or human, collects RSS samples to determine the AOA of the target. How should we design the rotating strategy so that RSS samples can reconstruct the target's transmission power distribution over the antenna's heading?*

Fig. 1 shows an example of the target power distribution $s(t)$ over the antenna's heading. A directional antenna is placed at position A. Dots around $s(t)$ refer to RSS samples collected by the sniffer when the directional antenna rotates to that direction. The LOS path is represented by segment AB. Ideally, if the antenna rotates slowly enough and collects at least one RSS sample when the antenna rotates to the LOS direction, then the peak of $s(t)$ corresponds to the LOS direction, and AOA is correctly measured. However, an extreme counterexample is that if the antenna rotates one round per second and the target is transmitting 1 packet per second, we cannot reconstruct the target power distribution s(t) over antenna's heading. In reality, it is highly possible that the packet transmission rate of a target (e.g. a laptop) may be quite slow or irregular. Hence, a careful control of the antenna's rotation is necessary. We will present our solution to adjusting the antenna's rotation in Section IV.

IV. RSS Sampling Theory for Accurate Wireless Localization

In this section, we present our theory on controlling rotation of a directional antenna, reconstructing the target's transmission power distribution over the antenna's heading and measuring AOA. Three cases are considered: (i) The rotation speed of the antenna is adjustable and wireless packet arrival follows a Poisson process; (ii) The rotation speed is fixed and packet arrival follows a Poisson process; (iii) The rotation speed of the antenna is either fixed or adjustable and **packet arrival is unpredictable**. All the three cases have their real-life incarnation.

A. Case I: Antenna with Variable Angular Velocity

Our analysis starts from the first case. We try to set an appropriate angular velocity so that the antenna is able to capture packets with the strongest signal strength in one round of rotation. Please note: once the angular velocity is determined, it will not change during rotation. As the antenna rotates, it keeps sniffing wireless traffic sent from the target. During one round of rotation, we denote the signal strength readings over time as $s(t)$, which can be treated as a continuous function with a baseband bandwidth f_{max}. f_{max} refers to the upper cutoff frequency and the positive-frequency range of significant energy of $s(t)$ is (0, f_{max}). **For conciseness of our statement, we will use bandwidth instead of baseband bandwidth hereafter**. In order to derive the line-of-sight angle between the antenna and the target, we should rotate the antenna at a reasonable slow speed but still efficient in time. Theorem 1 shows how to set the angular velocity w. Please refer to Appendix A for the proof.

Theorem 1. *Assume that the directional antenna rotates at an angular velocity w. Packets sent from a target mobile device in a unit time is modeled as a Poisson process with a rate of λ. Collected RSS samples can be used to reconstruct the target power distribution over the antenna's heading with a certainty of over 99% via one round of rotation if and only if the following condition is satisfied,*

$$P_r(w, \lambda, F_s) > 0.99, \tag{4}$$

where $P_r(w, \lambda, F_s)$ is defined as follows.

$$P_r(w, \lambda, F_s) = (1 - e^{-\frac{\lambda}{F_s}})^{\frac{2\pi F_s}{w}}, \tag{5}$$

$$F_s > 2f_{max}, \tag{6}$$

where F_s is the sampling rate, and f_{max} is $s(t)$'s bandwidth.

We make the following observations from Theorem 1.

- When other parameters are fixed, the higher the angular velocity w, the lower $P_r(w, \lambda, k)$.
- When other parameters are fixed, the higher λ, the higher $P_r(w, \lambda, k)$.
- When other parameters are fixed, the higher k, the lower $P_r(w, \lambda, k)$.

B. Case II: Antenna with Fixed Angular Velocity

If the rotation speed is fixed, we cannot adjust the speed to meet the Nyquist sampling theorem. However, we can rotate the antenna for several rounds. Theorem 2 illustrates how to estimate the minimum number of rounds that is needed for our sniffing.

Theorem 2. *Assume that it takes time T for the antenna to rotate for one round. The number of packets sent from a target device in a unit time is modeled as a Poisson process with a rate of λ. R is the number of rotations. The collected RSS samples can be used to reconstruct the target power distribution over antenna's heading with a certainty of over 99% via R rounds of rotations if and only if the following condition is satisfied,*

$$P_r(R, \lambda, F_s) > 0.99, \tag{7}$$

where $P_r(R, \lambda, F_s)$ is defined as follows.

$$P_r(R, \lambda, F_s) = (1 - e^{-\frac{R\lambda}{F_s}})^{TF_s}, \tag{8}$$

$$F_s > 2f_{max}, \tag{9}$$

where f_{max} is the bandwidth of $s(t)$.

We make the following observations from Theorem 2.

- (i) When other parameters are fixed, the more rounds of rotation, the higher $P_r(R, \lambda, F_s)$.
- (ii) When other parameters are fixed, the higher λ, the higher $P_r(R, \lambda, F_s)$.
- (iii) When other parameters are fixed, the higher F_s, the lower $P_r(R, \lambda, F_s)$.

C. Case III: Unpredictable Wireless Packet Arrival

Now we loose the assumption of packet transmission distribution. We assume that the angular velocity of the directional antenna is either adjustable or not and the antenna should be able to stop when instructed so. To guarantee that the RSS samples are correctly collected, we propose Theorem 3.

Theorem 3. *RSS samples can reconstruct the target power distribution over antenna's heading if and only if the angular sampling interval S_I (in degrees) satisfies (10) and a RSS sample must be collected within each S_I,*

$$S_I = \frac{1}{F_s}, \tag{10}$$

$$F_s > 2f_{max}, \tag{11}$$

where f_{max} is the band limit of the antenna gain pattern $g(\theta)$.

Proof: The antenna radiation pattern is $g(\theta)$ and its cutoff frequency is f_{max}. Recall the equation $s(\theta) = P(d) + g(\theta)$ in (3). Since the distance between the target and the sniffer is fixed, $P(d)$ is constant. The variation of RSS reading $s(\theta)$ only depends on the antenna directive gain $g(\theta)$. Therefore, the cutoff frequency of the power distribution $S(\theta)$ over angle is the cutoff frequency of the antenna gain pattern $g(\theta)$.

To be able to reconstruct $S(\theta)$, from the Nyquist sampling theorem, we know that the sampling frequency F_s must satisfy the condition presented in Formula (11). F_s determines how many samples we should collect in a angle of one degree. Its reverse, sampling interval S_I, implies that at least one RSS sample should be collected each S_I degrees. ■

Theorem 3 tells us that to correctly collect RSS samples, the directional antenna should collect at least one packet in each S_I. The directional antenna should stop and wait for the wireless packet to arrive if it does not receive a packet in a sampling interval of S_I degrees. We can see that this strategy does not require us to know the target packet arrival pattern in advance.

D. Practical Consideration

1) Determine λ: In the first two cases of determining AOA, we need to know the rate of the Poisson process λ in order to determine the parameters of rotating the directional antenna. λ can be derived in real time. We can collect wireless traffic sent from the target mobile device over a period of time and use the average packet transmission rate as λ. People may argue that traffic transmission does not follow a Poisson process. Actually, we can easily extend Theorems 1 and 2 to other cases with different packet transmission models. For example, Corollary 1 addresses the case that a target device transmits packets at a constant rate r. Its proof is straightforward.

Corollary 1. *A target device transmits packets at a constant rate r. Collected RSS samples can be used to reconstruct the target power distribution over the antenna's heading if and only if the following condition is satisfied,*

$$r > 2f_{max}, \tag{12}$$

where f_{max} is $s(t)$'s bandwidth, which is determined by the directional antenna angular velocity w.

Proof: To be able to reconstruct $s(t)$, from the Nyquist sampling theorem, we know that the sampling frequency F_s must satisfy the condition $F_s > 2f_{max}$ presented in Formula (11). F_s determines how many samples we should collect in a unit time (e.g. one second). Hence, in one unit time, the number of packets transmitted from a target should be no less than F_s. Therefore, we have $r \geq F_s$. Finally, we derive the equation in (12). ■

In cases that the packet transmission model cannot be determined, we can still apply Theorem 3 to determine the target AOA.

2) Determine f_{max}: In Case I with an antenna with adjustable angular velocity, denote $s(t)$ as the RSS function in

terms of time t. We can apply the Fourier transform to $s(t)$ in order to determine f_{max}.

Now let's derive $s(t)$. Recall $s(\theta) = P(d)+g(\theta)$ in Equation (3), where θ is the antenna's heading. Given rotating speed w, we can derive (13),

$$s(t) = g(wt) + P(d), \tag{13}$$

where d is the distance between the antenna and the target and $P(d)$ can be treated as a constant.

We apply the Fourier transform to both sides of Formula (13) and have

$$F[s(t)] = F[g(wt) + P(d)], \tag{14}$$
$$S(j\Omega) = G(wj\Omega) + 2\pi\delta(j\Omega). \tag{15}$$

Since $P(d)$ is a constant, its transform is a delta function $2\pi\delta(j\Omega)$ whose value is zero everywhere except at the origin. This item is insignificant as we are interested in the part of domain where Ω is positive. Therefore, deriving f_{max} of $s(t)$ is equivalent to deriving f_{max} of $g(wt)$. Recall that $g(wt)$ is the antenna gain function in terms of wt.

Our solution to deriving f_{max} of $g(wt)$ is as follows. We choose an angular velocity w_o and apply the Fourier transform to $g(w_o t)$, and derive G(wjΩ). Next, we square the absolute of G(wjΩ) and choose the bandwidth f_o using Formula (16),

$$\lim_{\varepsilon->0}\int_{\varepsilon}^{f_o} |G(wj\Omega)|^2 d\Omega = 0.95 \lim_{\varepsilon->0}\int_{\varepsilon}^{+\infty} |G(wj\Omega)|^2 d\Omega. \tag{16}$$

Basically, f_o is the cutoff frequency within which accumulates 95% of the power of the antenna gain function.

Then, we refer to the scaling property of the Fourier transform and establish a model which defines f_{max} as angular velocity w varies. Formula (17) gives the scaling of $s(t)$ in time domain as w varies, and Formula (18) exhibits the scaling in frequency domain,

$$s(t) = s_o(\frac{wt}{w_o}), \tag{17}$$
$$S(j\Omega) = \frac{w_o}{w} S_o(\frac{w_o}{w} j\Omega). \tag{18}$$

Therefore,

$$f_{max} = \frac{w}{w_o} f_o \tag{19}$$

In Case II for an antenna with fixed angular velocity w, we can directly apply the Fourier transform to antenna gain function $g(wt)$, and determine its bandwidth f_{max}.

3) Rotation Scheme Selection Criteria: Each of the theorems we propose so far corresponds to a rotation scheme, respectively. Now, we will introduce the selection criteria of these schemes. The selection of these schemes depends on the type of target we aim to locate and type of antenna in use.

The type of targets can be divided into two groups according to their transmission pattern. The first group of targets has an irregular transmission pattern. This group includes devices such as laptops, tablets, PADs and PDAs. The arrival of packets from these devices is often unpredictable. Therefore, we can apply Theorem 3 to the AOA measurement. The angular velocity of our directional antenna has to be adjustable so that we can pause the rotation at any time until at least one RSS sample is collected within a sampling interval.

The second group of targets has a regular transmission. This group includes devices such as wireless routers, and smartphones in AP mode. These group of targets broadcast beacon frames at a fixed rate (e.g. 100 beacons/sec). In this case, the selection of rotation schemes depends on the type of antenna in use. If the rotation speed is fixed, then we can only choose the second scheme. Otherwise, if the rotation speed is controllable, we compare these two schemes and choose the one with less time cost. The reason is that, in reality, a mobile device may not remain radioactive for a long time. Hence, it is critical to rotate the antenna efficiently. The time cost T_{s1} of the first rotation mechanism is calculated in Formula (20).

$$T_{s1} = \frac{2\pi}{w}. \tag{20}$$

The time cost T_{s2} of the second rotation mechanism is calculated in Formula (21)

$$T_{s2} = TR. \tag{21}$$

V. Evaluation

We conducted extensive experiments to validate the proposed theorems. In this section, we first introduce the experiment setup and then present experimental results.

A. Experiment Setup

We have successfully applied our RSS sampling theory to BotLoc, a self-coordinated programmable robot armed with a directional antenna. We design several real-world experiments to verify our theory.

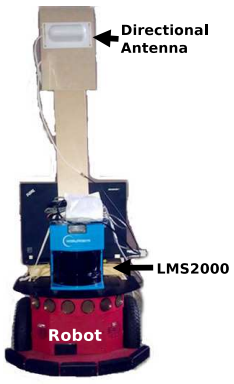

Fig. 2. Prototype

Fig. 2 shows a photo of the BotLoc prototype. BotLoc consists of two main components: (i) a robot, and (ii) a directional wireless sniffer. The robot is able to rotate after accepting heading commands from a software controller. This robot has an odometry coordinate system that keeps recording its odometric pose during rotations in terms of angle θ, and θ is the orientation of the robot with respect to its starting pose. The software controller also controls the directional wireless sniffer to collect RSS samples as a signal strength time series.

Therefore, we can rotate BotLoc and collect RSS samples simultaneously. When the rotation is finished, the software controller inspects the signal strength time series coupled with angle information in order to compute the target AOA.

BotLoc's hardware and software configuration is as follows. The robot we choose is *Pioneer P3-DX* [12], a remotely operated and programmable robot. P3-DX can be controlled by either a joystick or a program. The software controller runs on a Lenovo W500 laptop, and it uses an object-oriented, robot control applications-programming interface (ARIA) from the manufacturer to control the robot. A robot operator can launch a client program such as *MobileEyes* [11] to set up a TCP connection to the software controller, and execute AOA measurement for a specified target remotely.

The wireless sniffer is an AirPcap Nx 802.11 a/b/g/n USB Wireless Adapter with a external directional antenna. A wireless sniffing program is installed in the laptop to collect RSS samples. The directional antenna is a 2.4 GHz 5 dBi Patch Wide Angle Antenna [5] with a vertical beam width of 135 degrees and a horizontal beam width of 34 degrees. The radiation patterns of the antenna are illustrated in Fig. 3.

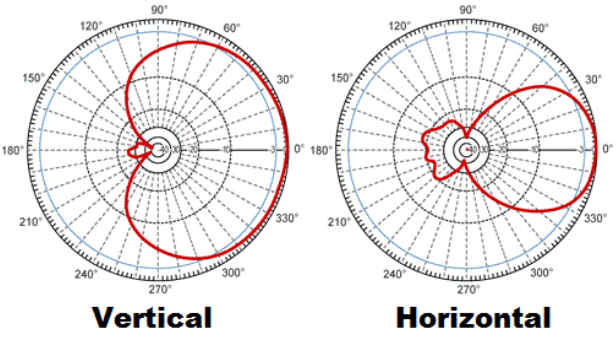

Fig. 3. Radiation Pattern of Directional Antenna in Use

We use a laptop that keeps sending out ICMP packets as a target mobile device, and its transmission rate follows the poisson distribution. We use BotLoc to identify the angle of arrival (AOA) from the target. We measure the accuracy of BotLoc via comparing the calculated AOA to the real AOA. To validate the correctness of our theorems, we select an open area with a direct line-of-sight path between the robot and the target. As discussed in previous section, this setup does not lose generality since measuring AOA in whatever condition is a basic problem.

B. Experimental Results

Before conducting the experiments, we need to calculate the sampling frequency. The sampling frequency is k (> 2) times the cutoff frequency of the directional antenna's radiation pattern. To derive the cutoff frequency of the antenna, we utilize the horizontal radiation pattern shown in Fig. 3. This radiation pattern can be treated as a signal power distribution $s(t)$ over time t at an angular velocity w_0 which is 1 deg/sec. Hence, we apply the Fourier transform to $s(t)$ and select a frequency as the cutoff frequency f_0 so that a large percentage (e.g. 95%) of the energy in the spectrum is preserved. Therefore, to derive the cutoff frequency f_{max} at any angular velocity w, we just apply w, f_0, and w_0 to the equation $f_{max} = \frac{w}{w_o} f_o$ in Formula (19). For the directional antenna installed in BotLoc, its cutoff frequency f_0 at 1 deg/sec is 0.22Hz.

1) Angular Velocity vs AOA Accuracy: To validate Theorem 1, we conducted two groups of experiments. In the first group of experiments, the target packet transmission follows a Poisson distribution with average rate of 80 ICMP packets per second. We rotate BotLoc at different angular velocities and detect the target AOA. Referring to Theorem 1, the angular velocity should not exceed 16 degree per second (deg/s), given the bandwidth of the directional antenna as 0.22 Hz. To compare the performance of AOA measurement below and above 16 deg/s, we set the angular velocity as 8, 12, 16, 20, 24, and 32 deg/s. For each velocity setting, we use BotLoc to measure target AOA for 20 times. To calculate the error between our measured AOA and the real AOA, we measure the real AOA via a Leica laser range finder [1]. We place the laser range finder on the top center of BotLoc and rotate BotLoc until the laser range finder points to the target. The angle with respect to the original direction is the target's real AOA. We present the experiment results in Figs. 4, 5.

In Fig. 4, the x-axis represents angular velocity of BotLoc, and the y-axis represents AOA accuracy measured in degree. From this figure, we have the following observations. (i) The mean of AOA error fluctuates around 0. (ii) When the angular velocity is below the threshold we calculated, that is 8, 12, or 16 deg/s, the mean of AOA measurement error is close to 0. When the angular velocity is 20 deg/s, which is slightly higher than our threshold, the mean of AOA measurement error is also close to 0. However, when the angular velocity is 24, or 32 deg/s, the mean of AOA error is comparatively far to 0. (iii) When the angular velocity is 8, 12, or 16 deg/s, the confidence interval of AOA error is narrow. On the other hand, when the angular velocity is 20, 24, or 32 deg/s, the confidence interval of AOA error is wide. From these observations, we conclude that when the angular velocity exceeds 16 deg/s, the accuracy of AOA measurement falls dramatically.

Fig. 5 shows the cumulative distribution of the angular error in AOA measurement at two different angular velocities. The x-axis is the absolute angular error between measured AOA and true AOA, and y-axis is the probability. There are two curves in the figure. The first curve is derived from one group of experiments conducted at a velocity of 8 deg/s, which is under the limitation of 16 deg/s from our theory. The second curve corresponds to another group of experiments conducted at a velocity of 20 deg/s, which is above the limitation of 16 deg/s. From this figure, we derive the following observations. (i) When the angular velocity is under the limitation, in 90% of experiments, the error of AOA measurement is no more than 20 degrees. (ii) When the angular velocity is above the limitation, only 50% of experiments produce an error of below 20 degree.

Fig. 4 and 5 verify that our mathematical model in Formula (4) is correct. To achieve high accuracy, the angular velocity should not exceed the threshold.

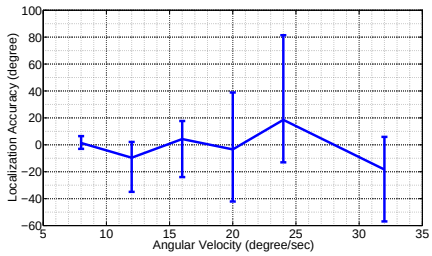

Fig. 4. Evaluation of Theorem 1: Angular Velocity vs AOA Accuracy

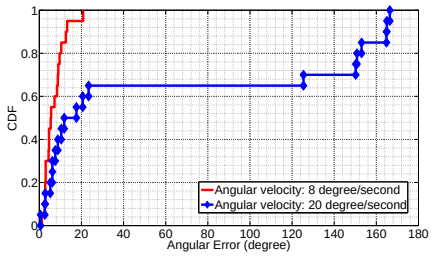

Fig. 5. Evaluation of Theorem 1: Comparison of AOA Accuracy with Different Angular Velocities

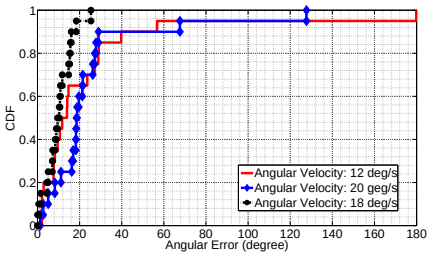

Fig. 6. Corridor case: Angular Velocity vs AOA Accuracy

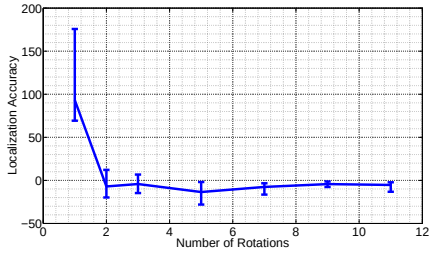

Fig. 7. Evaluation of Theorem 2: Number of Rotations vs AOA Accuracy

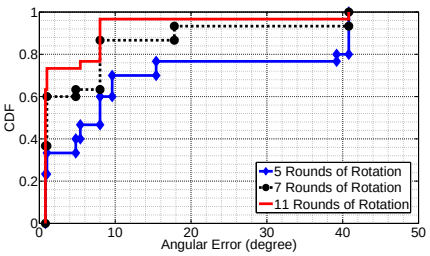

Fig. 8. Evaluation of Theorem 2: AOA Accuracy with Different Rounds of Rotations

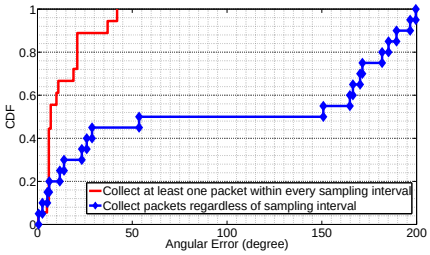

Fig. 9. Evaluation of Theorem 3: Sampling Interval vs AOA Accuracy

In the second group of experiments, we try to verify that only when the angular velocity is below the threshold is the velocity slow enough. Otherwise, even the antenna rotates slowly but faster than the threshold, the collection of RSS samples is still incorrect. In this group of experiments, we place the robot and the target in a corridor of our campus building, and there is a LOS path between them. However, sidewalls, chairs and tables induce signal fading and shadowing. First of all, we set the transmission interval of the target to follow the Poisson distribution so that the transmission interval on average is 1.25 second. Referring to Theorem 1, the angular velocity should not exceed 0.16 deg/s. We choose two angular velocities that are above the threshold and they are 12 and 20 deg/s. For each setting of velocity, we use BotLoc to measure the target AOA for 20 times. Next, as a comparison, we set the target transmission rate to be 100 pkt/s, and referring to our theory, the angular velocity should not exceed 20 deg/s. We set the angular velocity to 18 deg/s which is below the velocity boundary. We then repeat AOA measurements for 20 times. To derive the true AOA between the target laptop and BotLoc, we leverage the off-the-shelf SLAM function shipped with the robot to generate the map for the entire floor, therefore, each position in the floor corresponds to a unique pair of coordinates in the map. With the coordinates of the target and BotLoc, and the original direction of BotLoc, we can derive the true AOA with respect to the original direction of BotLoc.

Fig. 6 shows cumulative angular error in AOA estimation at three different angular velocities when the experiments are conducted in a corridor of our campus building. There are three curves in this figure. The first curve represents experimental results when the target transmission rate is 0.8 pkt/s and the robot rotates at 12 deg/s. The second curve represents experimental results when the target transmission rate is 0.8 pkt/s and the robot rotates at 20 deg/s. The third curve represents experimental results when the target transmission rate is 100 pkt/s and the robot rotates at 18 deg/s. From Fig. 6, we make the following observations: (i) When the angular velocity is above the threshold, the performance of the AOA measurement at 12 deg/s is not much better than 20 deg/s. (ii) When the angular velocity is below the threshold, the performance of the AOA measurement at 18 deg/s is better than the others. (iii) Even when the velocity 18 deg/s is much faster than 12 deg/s, it is still slow enough to derive a correct RSS collection. According to these observations, we conclude that: Theorem 1 provides a standard to define how slow is slow. Under a different target transmission rate, the velocity threshold is different. We cannot choose a slow velocity in a subjective way but we have to follow the standard in our theory.

2) Rounds of Rotations vs AOA Accuracy: To validate Theorem 2, we place BotLoc and the target in an open area with no obstacles around. We set the transmission rate of the target to follow the Poisson distribution so that the target keeps sending out 16 ICMP packets per second on average. We fix the angular velocity of BotLoc to 20 deg/s and measure the target AOA. Referring to Theorem 2, to correctly collect RSS samples, the number of rotations should be more than 7. To view the performance of AOA measurement, we set the rounds of rotations to 1, 2, 3, 5, 7, 9, 11. For each setting of rounds of rotations, we repeat the AOA measurement for 30 times. The experiment results are in Figs. 7 8.

Figs. 7, 8 exhibit the AOA accuracy versus different rounds

of rotations. In Fig. 7, The x-axis represents the number of rotations, and the y-axis represents error of AOA measurement in degree. From our calculation, the number of rotations should be at least 7 rounds. From this figure, we derive the following observations. (i) When the number of rotations is 1, 2, 3 or 5, the mean of AOA error is approaching but still away from 0. (ii) When the number of rotations is 7, 9, or 11, the mean of AOA error is close to 0. (iii) When the number of rotations increases, the confidence interval of AOA error becomes short. (iv) When the number of rotations is 7, 9 or 11, the confidence interval of AOA error is very short; however, when the number of rotations is 1, 2, 3 or 5, the confidence interval is relatively wide.

Fig. 8 illustrates the cumulative distribution of angular error in AOA measurement. There are three curves in this figure. The first curve represents AOA measurement using 11 rounds of rotations, and the second curve represents AOA measurement using 7 rounds of rotations. The third curve represents AOA measurement using 5 rounds of rotations. From this figure, we derive the following observations. (i) The first and second curves are relatively close to each other, which means that when the number of rotations are above the threshold, the AOA accuracy is similar. (ii) The third curve is relatively far from the others, which means that if the number of rotations is below the threshold, the accuracy is low. (iii) When the number of rotations is over the threshold, over 60% of experiments produce an accuracy of under 5 degrees. On the contrary, when the number of rotations is below the threshold, no more than 40% of experiments produce an accuracy of under 5 degrees.

According to these observations, we conclude that Theorem 2 is correct, and it provides a standard to determine how many rounds of rotations is enough. To decide how many rounds of rotations, we should consider the target transmission rate, antenna rotation period, and antenna radiation pattern.

3) Analysis of Angular Sampling Interval: To validate Theorem 3, we place BotLoc and a target in an open area with no obstacles nearby. We set the transmission interval of the target to follow the Poisson distribution so that the transmission interval on average is 2 seconds. As the bandwidth of the directional antenna is 0.22 Hz. Referring to Theorem 3, the sampling interval is 3 degrees. We rotate BotLoc to collect at least one packet within every 3 degrees, and repeat the experiment for 20 times. As a comparison, we randomly rotate the antenna and collect RSS samples, and we repeat this process for 20 times. The result is shown in Fig. 9.

Fig. 9 shows the cumulative distribution of angular error in AOA measurement. There are two curves in this figure. The first curve shows the AOA accuracy when we collect at least one packet within every angular sampling interval of 3 degrees, and the second curve shows the accuracy of AOA measurement when we randomly rotates the antenna and collect RSS samples. The x-axis represents the absolute angular error between the estimated AOA and the true AOA, and the y-axis represents the probability of angular error. From this figure, we observe that when the sampling process follow Theorem 3, the accuracy is much higher. This validates the correctness of Theorem 3.

VI. Conclusion

In this paper, we addressed a critical, but unanswered question: How can we use collected RSS samples by a rotating a directional antenna, carried by humans or vehicles, to reconstruct the target transmitters power distribution over antenna's heading in the space? With a reconstructed RSS distribution, we can derive AOA which corresponds to the angle at which the maximum RSS is measured.

We innovatively apply the Nyquist sampling theory to address this problem and develop a set of RSS sampling theory. We explicitly formulated the relationship among the directional antenna's radiation pattern, rotation angular velocity, and the target mobile's packet transmission interval. We developed a fully functional localization system: BotLoc. BotLoc is a P3-DX robot armed with a directional wireless sniffer. It applies our RSS sampling theory for collecting RSS samples and precisely measuring AOA. It is infrastructure-free and training-free. Our contribution also includes extensive experiments which demonstrate the effectiveness of the proposed theorems and system. We expect that our theory and system will provide a fundamental, empirical and theoretical guideline for AOA measurement with a rotating directional antenna.

References

[1] Leica disto d8, the versatile one for in- and outdoor. http://ptd.leica-geosystems.com/en/Laser-Distancemeter-Leica-DISTO-D8_78069.htm, 2009.

[2] P. Bahl and V. N. Padmanabhan. RADAR: An in-building RF-based user location and tracking system. In *Proceedings of INFOCOM*, 2000.

[3] Y. Chen, Z. Liu, Y. Ding, and X. Fu. On sampling signal strength for localization using a directional antenna. In *Proceedings of IEEE International Workshop on Data Security and PrivAcy in wireless Networks (D-SPAN)*, 2011.

[4] Y. Chen, D. Lymberopoulos, J. Liu, and B. Priyantha. Fm-based indoor localization. In *Proceedings of MobiSys*, June 2012.

[5] L. com Inc. Lcom antenna. http://www.l-com.com/productfamily.aspx?id=6533, 2012.

[6] P. Enge and P. Misra. Special issue on global positioning system. *Proceedings of the IEEE*, 87(1):3–15, January 1999.

[7] Fidelity Comtech, Inc. 802.11 phocus array antenna system by fidelity comtech. http://www.fidelity-comtech.com/, 2009.

[8] X. Fu, N. Zhang, A. Pingley, W. Yu, J. Wang, and W. Zhao. The digital marauders map: A new threat to location privacy in wireless networks. In *Proceedings of ICDCS*, 2009.

[9] D. Han, D. G. Andersen, M. Kaminsky, K. Papagiannaki, and S. Seshan. Access point localization using local signal strength gradient. In *Proceedings of Passive & Active Measurement (PAM)*, 2009.

[10] A. Harter, A. Hopper, P. Steggles, A. Ward, and P. Webster. The anatomy of a context-aware application. In *Proceedings of MOBICOM*, 1999.

[11] A. T. Inc. Mobileeyes. http://www.mobilerobots.com/ResearchRobots/PioneerSDK/MobileEyes.aspx, 2011.

[12] A. T. Inc. Pioneer p3-dx. http://www.mobilerobots.com/researchrobots/researchrobots/pioneerp3dx.aspx, 2011.

[13] K. Kawauchi, T. Miyaki, and J. Rekimoto. Directional beaconing: A robust wifi positioning method using angle-of-emission information. In *Proceedings of LoCA*, 2009.

[14] L. M. Ni, Y. L. Yiu, C. Lau, and A. P. Patil. LANDMARC: Indoor location sensing using active RFID. In *Proceedings of PerCom*, pages 407–415, 2003.

[15] D. Niculescu and B. Nath. VOR base stations for indoor 802.11 positioning. In *Proceedings of MOBICOM*, 2004.

[16] N. B. Priyantha, A. Chakraborty, and H. Balakrishnan. The Cricket Location-Support System. In *Proceedings of MOBICOM*, 2000.

[17] T. S. RAPPAPORT. *Wireless Communications: Principles and Practice (2nd Edition)*. Prentice Hall, 2002.
[18] K. Römer. The lighthouse location system for smart dust. In *Proceedings of MobiSys*, 2003.
[19] A. P. Subramanian, P. Deshpande, J. Gao, and S. R. Das. Drive-by localization of roadside wifi networks. In *Proceedings of INFOCOM*, 2008.
[20] H. Wang, S. Sen, A. Elgohary, M. Farid, M. Youssef, and R. R. Choudhury. No need to war-drive unsupervised indoor localization. In *Proceedings of MobiSys*, June 2012.
[21] J. Wang, Y. Chen, X. Fu, J. Wang, W. Yu, and N. Zhang. 3dloc: Three dimensional wireless localization toolkit. In *Proceedings of the 2010 IEEE 30th International Conference on Distributed Computing Systems*, ICDCS '10. IEEE Computer Society, 2010.
[22] R. Want, A. Hopper, V. Falcao, and J. Gibbons. The active badge location system. *ACM Transactions on Information Systems*, 10(1), January 1992.
[23] Z. Zhang, X. Zhou, W. Zhang, Y. Zhang, G. Wang, B. Y. Zhao, and H. Zheng. I am the antenna: accurate outdoor ap location using smartphones. In *Proceedings of the 17th annual international conference on Mobile computing and networking*, 2011.

APPENDIX A - PROOF OF THEOREM 1

Proof: The antenna rotates over 2π while it is sampling signal s(t). In order to determine AOA of the target signal transmission, we should be able to perfectly reconstruct s(t) from the sampled data without losing any knowledge of the peak of s(t). Therefore, this sampling process needs to satisfy the Nyquist sampling theorem, which means that the sampling rate F_s should be larger than twice of f_{max}.

Because the signal transmission process is discrete over time, so we can not guarantee that our sampling process fulfills the Nyquist sampling theorem even the sampling rate agrees with Formula (12) unless we are able to collect at least $\frac{2\pi F_s}{w}$ samples. To achieve this goal, we devide a rotation of 360 degree into $\frac{2\pi F_s}{w}$ sub processes. In any of these sub processes, the antenna turns over an arc of $\frac{w}{F_s}$. We denote the time at the beginning of the rotation as 0. We select the nearest neighbouring data from time interval [$\frac{i-1}{F_s}$, $\frac{i}{F_s}$] to represent the sample at time $\frac{i}{F_s}, i = 1, ..., \frac{2\pi F_s}{w}$. By the end of the rotation, the maximum signal strength readings might be collected as the Nyquist theorem is satisfied. However, this is not 100% for sure as the wireless signal transmission is a Poisson process with a rate of λ. At any period of time interval t (t = $\frac{1}{F_s}$), the probability that k packets are captured is estimated in Formula (22).

$$P[N(t) = k] = \frac{(\lambda t)^k}{k!} e^{-\lambda t}, t = \frac{1}{F_s}. \quad (22)$$

The probability that at least one packet is captured at any time interval t can be calculated in Formula (25).

$$\begin{aligned} P[N(t) \geq 1] &= 1 - P[N(t) = 0] && (23)\\ &= 1 - \frac{(\lambda t)^0}{0!} e^{-\lambda t} && (24)\\ &= 1 - e^{-\lambda t} && (25) \end{aligned}$$

Hence, we can deduct from Formula (25) and calculate the probability that at least $\frac{2\pi F_s}{w}$ packets are sampled after one round of rotation. Formula (30) shows the calculation.

$$\begin{aligned} P_r(w, \lambda, F_s) &= P[N(t) \geq 1]^{\frac{2\pi F_s}{w}} && (26)\\ &= (1 - P[N(t) = 0])^{\frac{2\pi F_s}{w}} && (27)\\ &= (1 - \frac{(\lambda t)^0}{0!} e^{-\lambda t})^{\frac{2\pi F_s}{w}} && (28)\\ &= (1 - e^{-\lambda t})^{\frac{2\pi F_s}{w}} && (29)\\ &= (1 - e^{-\lambda \frac{1}{F_s}})^{\frac{2\pi F_s}{w}} && (30) \end{aligned}$$

Hence, The proof is completed. ■

APPENDIX B - PROOF OF THEOREM 2

Proof: This proof is similar to the previous one. We divide a circle equally into TF_s pieces of arcs, each of which has a radian of $\frac{2\pi}{TF_s}$. Based on the Nyquist sampling theory, every time the antenna rotates over $\frac{2\pi}{TF_s}$, at least one packet should be captured. Due to the fixed rotation speed, this requirement is not always sufficed. A high rotation speed may lead to the fact that no packet is captured when the antenna rotates over certain arcs. We repeat the rotation for R rounds to raise the probability that at least one packet is captured when the antenna rotates over the ith arc (i=1,2,...,TF_s). As the arrival of every packet is independent, this probability is calculated using the following formula.

$$\begin{aligned} Pr(N_i(t)) &= 1 - \prod_{j=0}^{R-1} P[N(Tj + it) - N(Tj + it \\ &\quad -t) = 0], i = 1, 2..., TF_s; t = \frac{1}{F_s} && (31)\\ &= 1 - P[N(it + t) - N(it) = 0]^R && (32)\\ &= 1 - (\frac{(\lambda t)^0}{0!} e^{-\lambda t})^R && (33)\\ &= 1 - e^{-\lambda t R} && (34) \end{aligned}$$

Therefore, we are able to calculate the probability that at least one packet is captured for every arc after R rotations. We present our calculation in Formula (38).

$$\begin{aligned} P_r(R, \lambda, F_s) &= \prod_{i=1}^{TF_s} Pr(N_i(t)) && (35)\\ &= Pr(N_i(t))^{TF_s} && (36)\\ &= (1 - e^{-\lambda t R})^{TF_s} && (37)\\ &= (1 - e^{-\lambda \frac{R}{F_s}})^{TF_s} && (38) \end{aligned}$$

Hence, the proof is completed. ■